High-coherence fluxonium as a probe of D-Wave's QPU environment

WHITEPAPER

Summary

Fluxonium has become an attractive candidate qubit for all of D-Wave Quantum's technologies. D-Wave Quantum has fabricated 2-dimensional single fluxonium test circuits and has confirmed that their coherence is comparable to the state-of-the-art reported in the scientific literature. Moreover, the data from these qubits has revealed that the electromagnetic environment within D-Wave Quantum's cryogenic systems is comparable to the best results for superconducting qubits published to date.

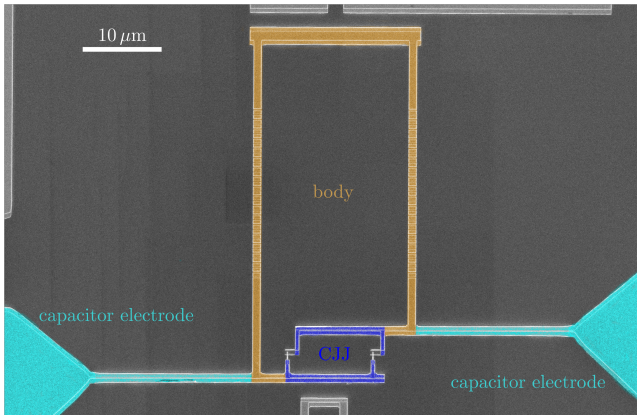

Figure 1: Scanning electron micrograph of a fluxonium qubit manufactured by D-Wave Quantum.

Introduction

D-Wave Quantum is primarily known for its quantum annealing (QA) technology based on superconducting flux qubits [1]. The energy spectrum of such a qubit is characterized by two low-energy states that are well separated from the higher energy states. The low-energy states can be described as tunable superpositions of two oppositely polarized magnetic moments, depending on the amount of magnetic flux threading through the body of the device. This qualitative description of the energy spectrum applies over a broad range of flux-like qubit designs [2–4].

Fluxonium [4] is a relatively modern member of the flux-like qubit family. This qubit is currently being considered for future gate model quantum computing (GMQC) technologies [5–8]. Fluxonium has at least three notable properties that make it attractive: First, fluxonium has produced record-setting relaxation (T_1) times in the realm of superconducting qubits [9]. Second, the large separation in energy between the low- and high-energy states protects against excitation out of the low-energy manifold, which is a problem known as state leakage [10]. Third, fluxonium can be operated at considerably lower frequency than other superconducting qubits, thus reducing control complexity.

Given the growing interest in fluxonium and D-Wave Quantum's deep experience in building flux-like qubit quantum technologies, we have embarked upon a research program that harnesses the unique properties of fluxonium for all of D-Wave Quantum's technology development. The primary impetus was to fabricate fluxonium to serve as a 'gold standard' high-coherence flux-like qubit that could be used to characterize D-Wave Quantum's QA quantum processing unit (QPU) electromagnetic environment. However, we are also using early generation fluxonium test circuits to validate potential use of fluxonium in future QA and GMQC technologies. This report summarizes some of the results obtained from single fluxonium circuits fabricated by D-Wave Quantum and measured within one of our QA QPU cryogenic systems. We observed that our fluxonium coherence times are comparable to the state-of-the-art reported in the scientific literature for 2-dimensional circuit geometries. We have also observed a very low effective qubit temperature that is among the best reported in the literature to date. This latter observation stands testament to the quality of the engineering that has gone into D-Wave Quantum's QPU environment.

Circuit

A scanning electron micrograph image of a fluxonium qubit manufactured by D-Wave Quantum is shown in Fig. 1. The qubit is composed of two closed superconducting loops: a large loop consisting of a so-called superinductor formed by two linear chains of nominally large Josephson junctions (JJs) and a second smaller loop containing two nominally small JJs. These loops are referred to as the body and compound Josephson junction (CJJ), respectively. Both loops can be flux biased by relatively slow baseband control lines. Only the body loop is subjected to fast small-amplitude control signals for qubit state manipulation. The qubit is capacitively coupled to a superconducting resonator that is used as a dispersive readout. The low-energy spectrum of the fluxonium shown is well characterized by an effective lumped element model [1] possessing body inductance $L_q = 250\,\mathrm{nH}$, body shunt capacitance $C_q = 6.5\,\mathrm{fF}$, and a maximum CJJ critical current $I_q^c = 28\,\mathrm{nA}$.

Coherence measurements

Qubit coherence was quantified using two standard metrics: relaxation time T_1 and Ramsey decay time T_{2R} [11]. For all results presented herein, the qubit was prepared in its ground state using a reset protocol and then adjusted to the target body and CJJ flux biases. State manipulation, evolution, and readout then followed. Measurements were obtained over a range of CJJ flux biases to adjust the energy spacing $E_q \equiv h\nu_\mathrm{q}$ between the two states in the low-energy manifold, where h is Planck's constant and ν_q is a frequency. All measurements were taken with the body flux bias tuned to the so-called degeneracy point where E_q is a minimum for a given CJJ bias. At this body flux bias, the ground and first excited state can be described as even and odd superpositions of oppositely polarized magnetic moments, respectively.

A summary of T_1 measurements versus ν_q is shown in the upper panel of Fig. 2. The measurements were taken with the cryogenic system stabilized at a temperature $T_\mathrm{env} = 7.3\,\mathrm{mK}$. The data exhibit scatter about a mean value of $\bar{T}_1 = 120\,\mu\mathrm{s}$ but otherwise a weak frequency-dependence. This is in contrast to the comparable results in [12] that exhibit a maximum $T_1 \sim 120\,\mu\mathrm{s}$ around $\nu_\mathrm{q} \approx 400\,\mathrm{MHz}$. This may be a signature of significantly lower flux noise in our qubit.

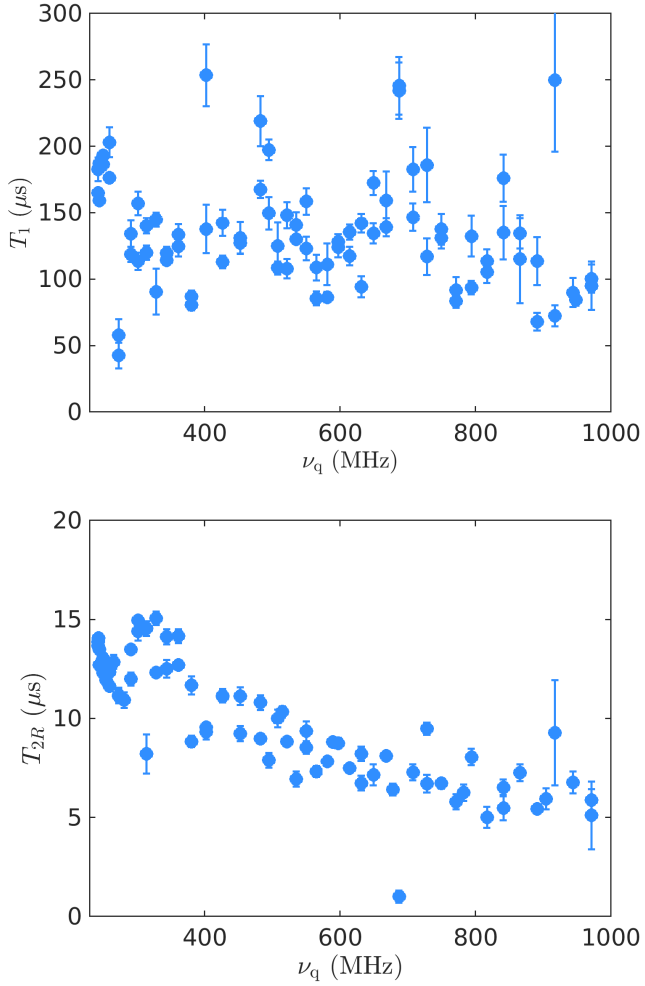

Figure 2: (Top) Relaxation time T_1 versus qubit frequency ν_q with the qubit at degeneracy. (Bottom) Ramsey dephasing time T_{2R} versus ν_q with the qubit at degeneracy. All measurements taken with the environment at temperature $T_\mathrm{env} = 7.3\,\mathrm{mK}$.

A summary of T_{2R} measurements versus ν_q is shown in the lower panel of Fig. 2. These data exhibit a monotonic dependence on qubit frequency, similar to what can be inferred from the data shown in [12]. The fact that $T_{2R} \ll 2T_1$ at all frequencies indicates that the qubit dephasing is dominated by very low frequency fluctuators. Furthermore, given that the largest values of T_{2R} are observed at low frequency, it can be argued that low frequency flux noise is not the dominant dephasing mechanism. Measurements using echo sequences are underway to gather further information.

Electromagnetic environment

A simple means to characterize a qubit's electromagnetic environment involves measuring the excited state probability once it has achieved steady state. This can be done, for example, by resetting the qubit in its ground state, applying a π-pulse to excite the qubit, and then letting the qubit evolve over many multiples of the relaxation time T_1 before measuring the final excited state probability. Alternatively, one could also reset the qubit, forgo the π-pulse and let the system be excited by the environment over many multiples of T_1 before measuring. Either way, the excited state probability must converge to a common steady-state value. That excited state probability can then be converted into an effective qubit temperature T_q under the assumption that the qubit has achieved thermal equilibrium with its environment. If one has an independent means to measure the temperature of the environment T_{env}, then the comparison between T_q and T_{env} yields useful information. If $T_q = T_{env}$ to within experimental resolution, then one can conclude that the electromagnetic environment contains negligible excess photons relative to the thermal background. If $T_q > T_{env}$, then the electromagnetic environment contains excess photons that must come from a source not at the temperature of the environment. The latter scenario must inevitably arise at very low T_{env} because the control lines reaching the qubit are capable of carrying energy from much higher temperature parts of the cryogenic apparatus down to the QPU space. Careful engineering is required to minimize this effect.

Figure 3 summarizes inferred values of T_q versus environment temperature T_{env} as obtained using the method described above with the qubit operated at $\nu_q = 715$ MHz. $T_q \approx T_{env}$ to within experimental error down to $T_{env} = 18$ mK, below which T_q saturates. For comparison, one can seek saturating values of T_q in the scientific literature for other superconducting qubits. Most notably, many researchers working with superconducting qubits report $T_q \gtrsim 30$ mK [3, 13, 14]. Note that all of these qubits were operated at considerably higher frequency than our device, typically close to 5 GHz, thereby necessitating a relatively large operating bandwidth for the bias lines. Increasing the bandwidth of the bias circuits inevitably leads to more noise reaching the qubit. Fluxonium circuits operated with such high bandwidths, both in 2-dimensional [8] and 3-dimensional [9] geometries, have yielded $T_q \gtrsim 25$ mK. A closer comparison is reported in [12] for a 2-dimensional fluxonium circuit operating within a similar frequency range as our qubit. Those authors quoted $T_q = 15$ mK, which is comparable to our result.

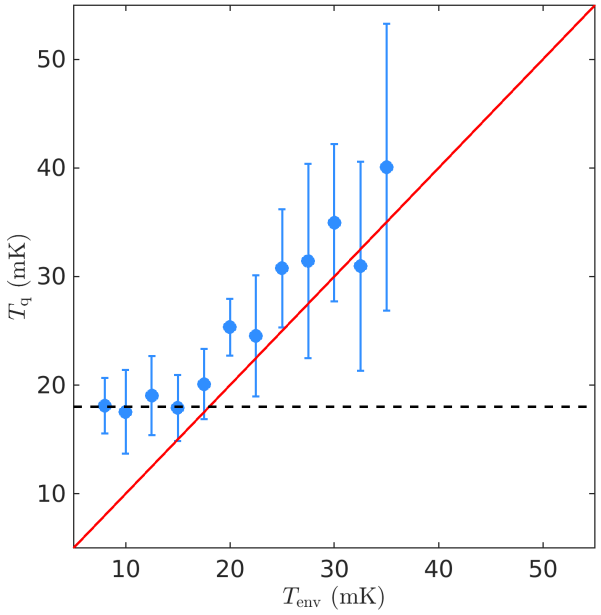

Figure 3: Inferred values of qubit temperature T_q versus environment temperature T_{env} for $\nu_q = 715$ MHz. T_q saturates at 18 ± 3 mK in the limit of low T_{env} as indicated by the dashed black line.

Next steps

While we primarily envisioned single fluxonium qubits serving as gold standards for testing our QA QPU electromagnetic environment, our experience has led us to believe that fluxonium could become the qubit of choice in future D-Wave Quantum technologies. Fluxonium is interesting from the perspective of QA when considering the trade-off between energy scale and coherence time [15]. It is likewise interesting from the perspective of GMQC as a means of addressing the known shortcomings of competing superconducting qubits such as the transmon. This relatively new qubit, coupled with D-Wave Quantum's deep expertise in engineering large-scale superconducting QPUs and their environments, will lead to exciting opportunities.

References

[1] R. Harris, J. Johansson, A. J. Berkley, M. W. Johnson, T. Lanting, et al., "Experimental demonstration of a robust and scalable flux qubit," Phys. Rev. B **81**, 134510 (2010).

[2] T. P. Orlando, J. E. Mooij, L. Tian, C. H. van der Wal, L. S. Levitov, S. Lloyd, and J. J. Mazo, "Superconducting persistent-current qubit," Phys. Rev. B **60**, 15398–15413 (1999).

[3] F. Yan, S. Gustavsson, A. Kamal, J. Birenbaum, A. P. Sears, et al., "The flux qubit revisited to enhance coherence and reproducibility," Nature Communications **7**, 12964 (2016).

[4] V. E. Manucharyan, J. Koch, L. I. Glazman, and M. H. Devoret, "Fluxonium: single cooper-pair circuit free of charge offsets," Science **326**, 113–116 (2009), eprint: `https://www.science.org/doi/pdf/10.1126/science.1175552`.

[5] F. Bao, H. Deng, D. Ding, R. Gao, X. Gao, et al., "Fluxonium: an alternative qubit platform for high-fidelity operations," Phys. Rev. Lett. **129**, 010502 (2022).

[6] L. B. Nguyen, G. Koolstra, Y. Kim, A. Morvan, T. Chistolini, et al., "Blueprint for a high-performance fluxonium quantum processor," PRX Quantum **3**, 037001 (2022).

[7] L. Ding, M. Hays, Y. Sung, B. Kannan, J. An, et al., *High-fidelity, frequency-flexible two-qubit fluxonium gates with a transmon coupler*, 2023, arXiv:2304.06087 [quant-ph].

[8] I. N. Moskalenko, I. A. Simakov, N. N. Abramov, A. A. Grigorev, D. O. Moskalev, A. A. Pishchimova, N. S. Smirnov, E. V. Zikiy, I. A. Rodionov, and I. S. Besedin, "High fidelity two-qubit gates on fluxoniums using a tunable coupler," npj Quantum Information **8**, 130 (2022).

[9] A. Somoroff, Q. Ficheux, R. A. Mencia, H. Xiong, R. Kuzmin, and V. E. Manucharyan, "Millisecond coherence in a superconducting qubit," Phys. Rev. Lett. **130**, 267001 (2023).

[10] B. M. Varbanov, F. Battistel, B. M. Tarasinski, V. P. Ostroukh, T. E. O'Brien, L. DiCarlo, and B. M. Terhal, "Leakage detection for a transmon-based surface code," npj Quantum Information **6**, 102 (2020).

[11] N. F. Ramsey, "A molecular beam resonance method with separated oscillating fields," Phys. Rev. **78**, 695–699 (1950).

[12] H. Sun, F. Wu, H.-S. Ku, X. Ma, J. Qin, et al., *Characterization of loss mechanisms in a fluxonium qubit*, 2023, arXiv:2302.08110 [quant-ph].

[13] X. Y. Jin, A. Kamal, A. P. Sears, T. Gudmundsen, D. Hover, et al., "Thermal and residual excited-state population in a 3D transmon qubit," Phys. Rev. Lett. **114**, 240501 (2015).

[14] C. M. Quintana, Y. Chen, D. Sank, A. G. Petukhov, T. C. White, et al., "Observation of classical-quantum crossover of $1/f$ flux noise and its paramagnetic temperature dependence," Phys. Rev. Lett. **118**, 057702 (2017).

[15] A. D. King, S. Suzuki, J. Raymond, A. Zucca, T. Lanting, et al., "Coherent quantum annealing in a programmable 2,000 qubit Ising chain," Nature Physics **18**, 1324–1328 (2022).